

# Water and Deuterium Oxide Permeability through Aquaporin 1: MD Predictions and Experimental Verification

Artem B. Mamonov,<sup>1</sup> Rob D. Coalson,<sup>1</sup> Mark L. Zeidel,<sup>2</sup> and John C. Mathai<sup>2</sup>

<sup>1</sup>Department of Chemistry and <sup>2</sup>Department of Medicine, University of Pittsburgh, Pittsburgh, PA 15260

Determining the mechanisms of flux through protein channels requires a combination of structural data, permeability measurement, and molecular dynamics (MD) simulations. To further clarify the mechanism of flux through aquaporin 1 (AQP1), osmotic  $p_f$  (cm<sup>3</sup>/s/pore) and diffusion  $p_d$  (cm<sup>3</sup>/s/pore) permeability coefficients per pore of H<sub>2</sub>O and D<sub>2</sub>O in AQP1 were calculated using MD simulations. We then compared the simulation results with experimental measurements of the osmotic AQP1 permeabilities of H<sub>2</sub>O and D<sub>2</sub>O. In this manner we evaluated the ability of MD simulations to predict actual flux results. For the MD simulations, the force field parameters of the D<sub>2</sub>O model were reparameterized from the TIP3P water model to reproduce the experimentally observed difference in the bulk self diffusion constants of H<sub>2</sub>O vs. D<sub>2</sub>O. Two MD systems (one for each solvent) were constructed, each containing explicit palmitoyl-oleoyl-phosphatidyl-ethanolamine (POPE) phospholipid molecules, solvent, and AQP1. It was found that the calculated value of  $p_f$  for D<sub>2</sub>O is ~15% smaller than for H<sub>2</sub>O. Bovine AQP1 was reconstituted into palmitoyl-oleoyl-phosphatidylcholine (POPC) liposomes, and it was found that the measured macroscopic osmotic permeability coefficient  $P_f$  (cm/s) of D<sub>2</sub>O is ~21% lower than for H<sub>2</sub>O. The combined computational and experimental results suggest that deuterium oxide permeability through AQP1 is similar to that of water. The slightly lower observed osmotic permeability of D<sub>2</sub>O compared to H<sub>2</sub>O in AQP1 is most likely due to the lower self diffusion constant of D<sub>2</sub>O.

## INTRODUCTION

Aquaporins belong to a family of membrane proteins that passively transport water, glycerol, and other small molecules (Nielsen et al., 2002). The archetypical water channel AQP1 has been shown to be highly specific for water and excludes protons, ammonia, and sugars such as glycerol (Zeidel et al., 1992, 1994). The specificity of the channel arises from the presence of two highly conserved NPA motifs (Asn-Pro-Ala residues) that form the narrow constriction of the pore region, which acts as a molecular sieve. Crystallographic studies suggest that the pore is narrow at the constriction and lets only water diffuse through it (Murata et al., 2000; Sui et al., 2001). Molecular dynamics (MD) simulation studies suggest the presence of another energy barrier that offers both steric and electrostatic selectivity, named the aromatic (ar/R) constriction, which is formed by the four amino acids Phe-56, His-180, Cys-189, and Arg-195 (rat AQP1) in water-selective aquaporins (de Groot et al., 2003; Chakrabarti et al., 2004; Chen et al., 2006). In aquaglyceroporins this constriction region is wider, as His-180 is usually replaced by Gly, which allows for water and glycerol to pass through as shown in GlpF (Fu et al., 2000).

Although general geometry of aquaporin channels differs only slightly between aquaporin family members, its water permeability may differ by several orders of magnitude. Water is thought to hydrogen bond to arginine in the NPA region (Miloshevsky and Jordan, 2004;

Vidossich et al., 2004) and the degree of hydrogen bonding or the energy barrier caused by hydrogen bonding is thought to dictate the rate of water flow through aquaporins. Furthermore, in a study of model channel desformylgramicidin, which shows a 100-fold increase in water permeability compared with gramicidin A, the lowered hydrogen bond-mediated energy barrier is thought to be responsible for large differences observed in water permeability (de Groot et al., 2002).

To determine whether such a finely tuned water channel allows the passage of deuterium oxide (D<sub>2</sub>O), a close analogue of water, we measured the permeability of D<sub>2</sub>O in AQP1-reconstituted proteoliposomes. D<sub>2</sub>O differs from H<sub>2</sub>O in the following respects: D<sub>2</sub>O has a lower zero-point vibrational energy leading to a stronger O-D bond and a stronger deuterium bond compared with the H-bond (Scheiner and Cuma, 1996). The effect of the stronger deuterium bond plus the heavier mass of D is believed to result in a self diffusion coefficient of D<sub>2</sub>O that is 18.6% lower than that of water (Mills, 1973; Grigera, 2001). Since water is thought to interact with specific residues Phe-56 and Arg-195 in the pore via hydrogen bonding (Miloshevsky and Jordan, 2004), it would be interesting to study the passage of D<sub>2</sub>O, which has a stronger deuterium bond. To test if kinetics of D<sub>2</sub>O permeability is different from H<sub>2</sub>O we

Correspondence to John Mathai: jmathai@bidmc.harvard.edu

Abbreviations used in this paper: AQP1, aquaporin 1; MD, molecular dynamics.

simulated D<sub>2</sub>O flux and then measured it, allowing us to determine the predictive power of MD simulations. Both MD simulations and experimental results indicate that D<sub>2</sub>O and H<sub>2</sub>O permeate AQP1 at similar rates.

## MATERIALS AND METHODS

### MD Simulations

Molecular dynamics (MD) simulations were used to calculate the diffusion and osmotic permeability of H<sub>2</sub>O and D<sub>2</sub>O through AQP1. The X-ray structure of bovine AQP1 was downloaded from the Protein Data Bank ([www.rcsb.org](http://www.rcsb.org)) with pdb code 1J4N (Sui et al., 2001). The tetrameric structure was assembled from the coordinates of the monomer using transformation matrices provided in the pdb file. The tetramer was then embedded in a pre-equilibrated patch of 177 palmitoyl-oleoyl-phosphatidyl-ethanolamine (POPE) molecules and solvated by 15,079 CHARMM modified TIP3P water molecules (Jorgensen et al., 1983; Neria et al., 1996) (referred to here as TIP3P), so that the total system contained 80,434 atoms. This system was energy minimized and equilibrated for 3 ns at 298 K and 1 atm. To construct the AQP1/D<sub>2</sub>O system, the TIP3P water model was replaced with a TIP3P-HW model (described below) and equilibrated for 1 ns at 298 K and 1 atm. The system equilibrium was checked by monitoring potential energy and volume over the course of the simulation. The standard deviation of potential energy from the mean was ~0.13% (~210 kcal/mol) and for volume was ~0.15% (~1150 Å<sup>3</sup>), which suggests that the system is in equilibrium.

Diffusion permeabilities were calculated for both AQP1/H<sub>2</sub>O and AQP1/D<sub>2</sub>O systems from equilibrium MD simulations at constant volume and constant temperature of 298 K from 31 and 26 ns trajectories, respectively. A weak harmonic restraining potential of 0.12 kcal/mol/Å<sup>2</sup> was applied in all three dimensions to AQP1 backbone α carbons to prevent the protein from drifting. Diffusion permeability was calculated using the following equation (Zhu et al., 2004):

$$p_d = \frac{V_W}{N_A} q_0 = v_w q_0, \quad (1)$$

where  $p_d$  (cm<sup>3</sup>/s/pore) is the diffusion permeability coefficient per pore,  $V_W$  is the molar volume of the solvent,  $N_A$  is Avogadro's number,  $q_0$  is the unidirectional permeation rate, and  $v_w$  is the volume of a single solvent molecule.  $q_0$  was calculated by counting the number of H<sub>2</sub>O or D<sub>2</sub>O molecules passing from one side of the channel to the other per unit time. The pore region was chosen to be the narrow central section of the channel, 22 Å in length, where water molecules pass in single file or nearly single file fashion (see Fig. 3, below).

Osmotic permeabilities were calculated by following the non-equilibrium MD method described by Zhu et al. (2004). A hydrostatic pressure gradient was established across the membrane by applying extra force to a layer of solvent molecules parallel to the membrane interface. Applied pressure MD simulations of different time length were performed at 25, 50, 100, and 200 MPa for both AQP1/H<sub>2</sub>O and AQP1/D<sub>2</sub>O systems. A force of 0.013445, 0.02689, 0.05378, and 0.10756 kcal/mol/Å was applied to oxygen atoms of H<sub>2</sub>O/D<sub>2</sub>O within an 8-Å solvent layer to generate 25, 50, 100, and 200 MPa pressure, respectively.

To prevent the protein and the lipid bilayer from moving under the influence of this external force, a harmonic restraint of 0.12 kcal/mol/Å<sup>2</sup> was applied in all three dimensions to the backbone α carbons of the protein and a harmonic restraint of 0.8 kcal/mol/Å<sup>2</sup> to the phosphorus atoms of the POPE molecules. This procedure differs somewhat from the 1D restraining procedure

used by Zhu et al. (2004). However, our calculated osmotic permeability for H<sub>2</sub>O turned out to be similar to Zhu et al. (2004) (see below), implying that small differences in the restraining procedure do not have a major effect on the calculated osmotic permeabilities.

The net flux of H<sub>2</sub>O/D<sub>2</sub>O through AQP1 was calculated by averaging the number of molecules that crossed three planes located 5 Å away from each other inside the channel per pore per unit time. Osmotic permeabilities were calculated from the slope of the best (linear least squares) fit line of H<sub>2</sub>O/D<sub>2</sub>O flux versus applied hydrostatic pressure according to the following equation (Zhu et al., 2004):

$$p_j = \frac{j}{\Delta P} k_B T, \quad (2)$$

where  $p_j$  (cm<sup>3</sup>/s/pore) is the osmotic permeability coefficient per pore,  $j$  (molecules/s) is the net solvent flux through a single water channel,  $\Delta P$  is the applied hydrostatic pressure,  $k_B$  is the Boltzmann constant, and  $T$  is the absolute temperature.

For our MD simulations we used the CHARMM 27 force field (MacKerell et al., 1998), which was derived to be consistent with the TIP3P model (Neria et al., 1996). For the parameterization of deuterium oxide we started with the TIP3P model as a reference, doubled the mass of the hydrogen atoms, and adjusted the partial charges of both the deuterium and oxygen atoms. The physical motivation for modifying these partial charges is to take into account the quantum effect that liquid D<sub>2</sub>O is characterized by a stronger deuterium bond than the H bond found in liquid H<sub>2</sub>O. This quantum effect arises because D<sub>2</sub>O has a lower zero-point vibrational energy than H<sub>2</sub>O (Scheiner and Cuma, 1996). It is well known that TIP3P water considerably overestimates (by more than a factor of 2) the self diffusion constant of water (van der Spoel et al., 1998; Mark and Nilsson, 2001). For this reason, we chose as a target for parameterization to reproduce the experimentally measured 18.6% difference in the self diffusion constants of H<sub>2</sub>O vs. D<sub>2</sub>O (Mills, 1973) rather than the experimental self diffusion constant of heavy water. A similar reparameterization of the SPC/E model for deuterium oxide has been reported recently in which only the mass and partial charges of the hydrogen atoms were changed in order to reproduce the experimental self diffusion constant, the molar volume and the potential energy of heavy water (Grigera, 2001). For our reparameterization, a simulation box of 3921 TIP3P water molecules was constructed, energy minimized, and equilibrated at 298 K and 1 atm. The mass of hydrogen atoms was set to 2 amu and atomic partial charges were incremented by fractions of a percent. The system was equilibrated for 0.5 ns followed by 1 ns production runs performed at a constant temperature of 298 K and a constant pressure of 1 atm. The self diffusion constant was calculated from the collected coordinate time series using the mean-square-displacement method (Allen and Tildesley, 1987). Adjustment of D<sub>2</sub>O atomic partial charges along with recalculation of the self diffusion constant was repeated until we generated a diffusion coefficient ~18% smaller than the value obtained with TIP3P under the same conditions.

All MD simulations were performed using the NAMD package (Kale et al., 1999) version 2.5. For long range electrostatics, the Particle Mesh Ewald method (Essmann et al., 1995) was used as implemented in the NAMD program along with periodic boundary conditions. The MD time step was set to 2 fs and the bonds between each hydrogen atom and its mother atom were fixed via the SHAKEH algorithm (Kale et al., 1999) to the nominal bond length given in the parameter file. MD coordinates of AQP1 simulations were saved every 1 ps and for the parameterization of TIP3P-HW water model every 100 fs. Most simulations were performed on Lemieux supercomputer at the Pittsburgh Supercomputing Center ([www.psc.edu](http://www.psc.edu)). It took ~4.6 h to run 1 ns of AQP1 simulations on 160 CPUs of Lemieux. All visualizations

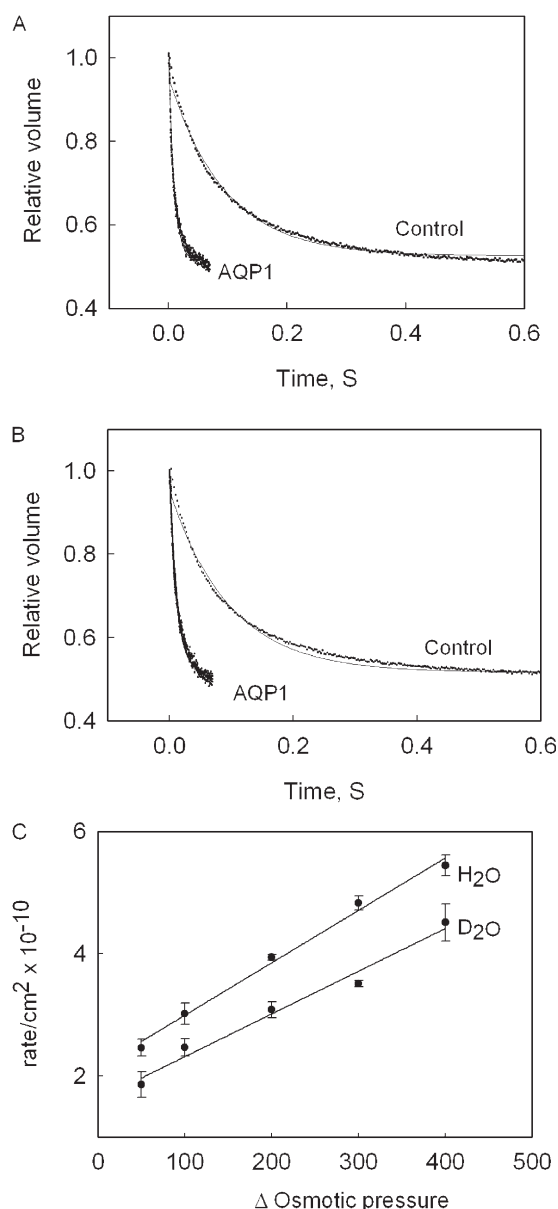


**Figure 1.** Osmotic permeability of H<sub>2</sub>O and D<sub>2</sub>O. Shown is the time course of volume change of AQP1-containing vesicles and control lipid vesicles on abrupt exposure to a doubling of external osmotic pressure in H<sub>2</sub>O (A) and D<sub>2</sub>O (B). C shows the effect of varying osmotic pressure (mOsm/kg) on permeability of H<sub>2</sub>O and D<sub>2</sub>O through AQP1.

and analysis of MD trajectories were made with the VMD program (Humphrey et al., 1996).

#### Reconstitution of AQP1 into Liposomes

Bovine AQP1 was purified from bovine red blood cells using methods similar to that used for purifying human AQP1 (Zeidel et al., 1992). The AQP1 reconstitution procedure was similar to that described earlier (Zeidel et al., 1994). In brief, 6–8 mg of palmitoyl-oleoyl-phosphatidylcholine (POPC) lipids (Avanti Lipids) was bath sonicated for three cycles of 3 min duration at 4 mW setting in 20 mM MOPS, pH 7.4. *N*-octylglucoside (OG) was added to the sonicated lipids to achieve a final concentration of 1.2% (vol/vol). To this, 50–60 μg of AQP1 in 1.5% OG was added and

incubated for 30 min on ice. The mixture was diluted 25-fold into reconstitution buffer (150 mM NaCl, 20 mM MOPS, pH 7.4) containing 10 mM carboxyfluorescein (CF). The proteoliposomes formed were collected by centrifugation at 100,000 *g* for 1 h. The external CF was removed by two additional centrifugal washes. The final pellet was resuspended in 300 μl of reconstitution buffer and used for permeability studies.

#### Measurement of Osmotic Permeabilities

Macroscopic osmotic permeabilities ( $P_f$ ) of H<sub>2</sub>O and D<sub>2</sub>O were measured as described earlier (Zeidel et al., 1994). In brief, the proteoliposomes were subjected to a doubling of external osmotic pressure in a stopped-flow fluorimeter (Applied Photophysics, SX.17 MV), and the fluorescence decrease of carboxyfluorescein due to self quenching caused by shrinkage of the vesicle was measured as a function of time. The data were fit using a single exponential function.  $P_f$  was calculated by comparing the single-exponential time constants fitted to a family of simulated curves generated using the water permeability equation in which  $P_f$  was varied to that obtained experimentally. MathCad was used to numerically integrate the water permeability equation:

$$\frac{dV_r(t)}{dt} = P_f \times r_{sv} \times V_w \times \left( \frac{C_{in}}{V_r(t)} - C_{out} \right). \quad (3)$$

In Eq. 3,  $V_r(t)$  is the relative volume of the vesicle at time  $t$  (i.e., volume at time  $t$ , divided by the initial volume),  $P_f$  (cm/s) is the macroscopic osmotic water permeability coefficient,  $r_{sv}$  is the surface area to volume ratio of a vesicle, and  $C_{in}$  and  $C_{out}$  are initial solute concentrations inside and outside the vesicle, respectively. The size of the vesicle was measured by laser light scatter using a DynaPro particle sizer. All other chemicals were obtained from Sigma-Aldrich.

## RESULTS AND DISCUSSION

Earlier studies before discovery of aquaporins showed that permeation of D<sub>2</sub>O across erythrocytes and red cell ghosts was inhibited by mercury (Karan and Macey, 1980; Ye and Verkman, 1989). However, mercurial compounds are nonspecific and do not inhibit the AQP1 channel completely (Zeidel et al., 1992). In this study we have performed a quantitative permeability measurement using purified AQP1, reconstituted into proteoliposomes, which eliminates the background permeability due to other proteins (Roudier et al., 1998; Yang et al., 2001). Fig. 1 shows the time course of relative volume change of liposomes on application of an osmotic gradient, causing the efflux of H<sub>2</sub>O (Fig. 1 A) or D<sub>2</sub>O (Fig. 1 B). It was found that the measured osmotic permeability of D<sub>2</sub>O ( $1.8 \times 10^{-2} \pm 0.42 \times 10^{-2}$  cm/s) is ~21% lower than that for H<sub>2</sub>O ( $2.3 \times 10^{-2} \pm 0.310^{-2}$  cm/s). This difference in permeability can be attributed to the higher viscosity of D<sub>2</sub>O vs. H<sub>2</sub>O and an 18.6% lower self diffusion coefficient of D<sub>2</sub>O compared with that of

TABLE I  
Force Field Parameters of TIP3P-HW Model

$r_{min}^{OO}$	$r_{min}^{DD}$	$\epsilon^{OO}$	$\epsilon^{DD}$	$q^O$	$q^D$	$b^{OD}$	$\theta^{DOD}$
Å	Å	kcal/mol	kcal/mol	<i>e</i> units	<i>e</i> units	Å	deg
3.5365	0.449	0.1521	0.046	-0.842	-0.421	0.9572	104.52

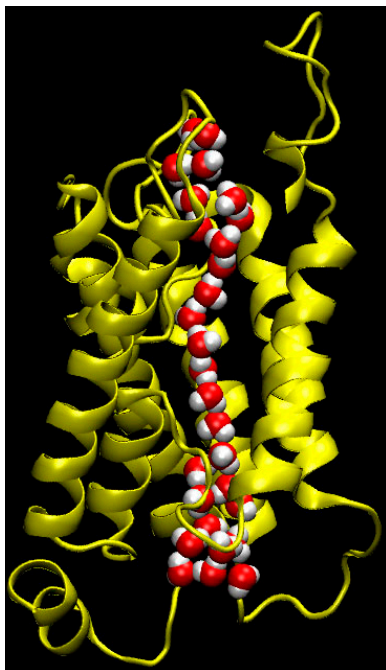


**Figure 2.** A snapshot from MD simulation of AQP1/H<sub>2</sub>O system. Only one monomer of the water channel is shown for clarity. Note the single file arrangement of water molecules inside the channel.

water (Mills, 1973). In red blood cells, before discovery of aquaporins, the decreased permeability of D<sub>2</sub>O was attributed to higher viscosity of D<sub>2</sub>O (Karan and Macey, 1980). A similar decrease of conductance of D<sub>2</sub>O through gramicidin was also attributed to higher viscosity of D<sub>2</sub>O (Tredgold and Jones, 1979). The background osmotic permeabilities of H<sub>2</sub>O and D<sub>2</sub>O in the absence of a water channel through POPC lipid membranes are 0.0032 cm/s and 0.0034 cm/s respectively. To confirm that the observed difference in permeability is not an isotope effect, we measured the osmotic permeability of AQP1 at various osmotic pressure values. Fig. 1 C shows that there is a linear increase in rate of efflux of H<sub>2</sub>O and D<sub>2</sub>O with increasing osmotic pressure. Furthermore the efflux of H<sub>2</sub>O and D<sub>2</sub>O shows a parallel increase with increasing osmotic pressure, suggesting that there are no additional interactions between the permeant and the channel as flux increases at higher osmotic pressures.

The force field parameters of our TIP3P-HW (D<sub>2</sub>O) model are summarized in Table I. Partial atomic charges are 0.96% higher compared with the TIP3P model.

TABLE II  
Results of Equilibrium MD Simulations

Time	No. of permeations	$q_0$	$p_d \times 10^{14}$
<i>ns</i>		<i>molecules/ns/pore</i>	<i>cm<sup>3</sup>/s/pore</i>
H <sub>2</sub> O	31.1	71	0.29 ± 0.026
D <sub>2</sub> O	26.3	65	0.31 ± 0.085
			0.85 ± 0.078
			1.0 ± 0.28

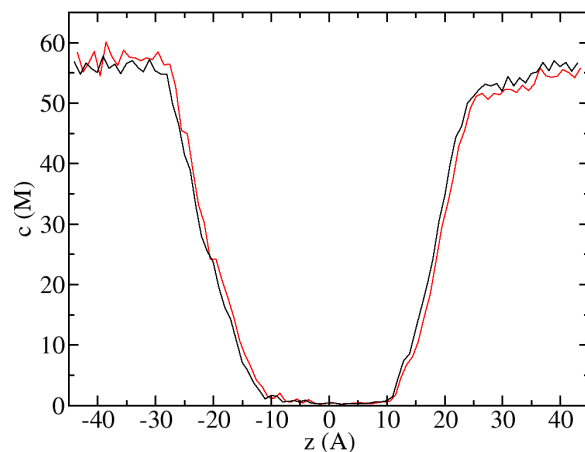


**Figure 3.** Concentration profile of H<sub>2</sub>O along z axis (channel axis) at equilibrium conditions (black line) and 100 MPa applied hydrostatic pressure (red line). Note the low concentration region between approximately  $z = -11 \text{ \AA}$  and  $z = +11 \text{ \AA}$ ; this is the “channel pore region” discussed in the text. Left side corresponds to cytoplasmic side.

This implies a larger dipole moment of  $7.904 \times 10^{-30}$  Cm which is also 0.96% larger than for the TIP3P model. The dimer potential energy in the most favorable configuration is  $-6.759$  kcal/mol, which is 2.4% larger in magnitude than for the TIP3P model. The heat of vaporization for TIP3P-HW is 10.68 kcal/mol, which is 2.9% larger than for the TIP3P model and compares well with the experimentally determined value of 11.11 kcal/mol for D<sub>2</sub>O (Nemethy and Scheraga, 1964). In our MD simulations, the TIP3P-HW model was characterized by a bulk diffusion coefficient of  $4.00 \times 10^{-5}$  cm<sup>2</sup>/s, which is 18.7% lower than that of the TIP3P model of water ( $4.92 \times 10^{-5}$  cm<sup>2</sup>/s). This difference is in good agreement with the experimentally measured difference of 18.6% between H<sub>2</sub>O and D<sub>2</sub>O (Mills, 1973). The densities of TIP3P and TIP3P-HW models were found to be 1.00 g/cm<sup>3</sup> and 1.13 g/cm<sup>3</sup>, respectively. This is also in good agreement with experimental densities of 0.997 g/cm<sup>3</sup> for H<sub>2</sub>O and 1.104 g/cm<sup>3</sup> for D<sub>2</sub>O (Weast, 1977). These solvent models were subsequently used to calculate the osmotic and diffusion permeabilities of H<sub>2</sub>O and D<sub>2</sub>O in AQP1.

A snapshot of the AQP1/H<sub>2</sub>O system from the equilibrium MD trajectory is presented in Fig. 2, with only one

TABLE III  
Results of Applied Pressure MD Simulations for H<sub>2</sub>O

Applied pressure	Time	No. of H <sub>2</sub> O permeations	Flux	$p_f \times 10^{14}$
<i>MPa</i>	<i>ns</i>		<i>H<sub>2</sub>O/ns/pore</i>	<i>cm<sup>3</sup>/s/pore</i>
25	8	21	0.65	
50	26.8	107	1.0	
100	21.9	171	1.9	10.0 ± 0.56
200	22	455	5.2	

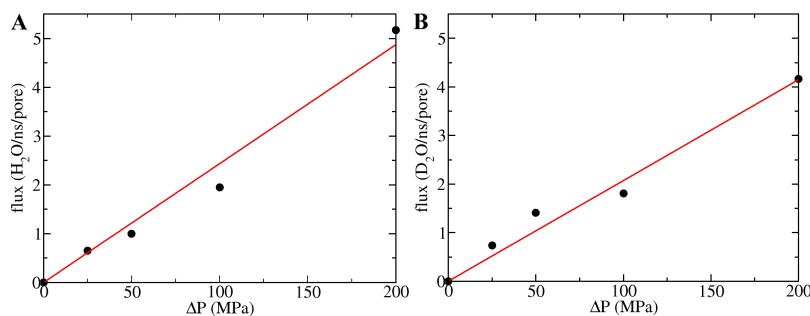


**Figure 4.** Computed flux versus applied hydrostatic pressure for H<sub>2</sub>O (A) and D<sub>2</sub>O (B). Circles (black) represent the calculated (average) data point values, which are shown along with the best-fit line (red). Standard error for the best fit line for H<sub>2</sub>O is 5.6% and for D<sub>2</sub>O 5.3%.

monomer and channel shown for the sake of clarity. The single file arrangement and rotation of the orientation of the water dipole, which are unique properties of the AQP family (de Groot and Grubmuller, 2001; Tajkhorshid et al., 2002), are correctly reproduced in our simulations. The single file channel occupancy for H<sub>2</sub>O and D<sub>2</sub>O are 9.7 and 9.5 molecules, respectively. The concentration profile of H<sub>2</sub>O across the channel system at equilibrium conditions is compared in Fig. 3 with that obtained at 100 MPa applied hydrostatic pressure. When hydrostatic pressure was applied, the concentration of water became slightly higher on the left side and lower on the right side of the membrane due to the compressibility of water. The main results of our equilibrium MD simulations for H<sub>2</sub>O and D<sub>2</sub>O are summarized in Table II. The unidirectional permeation rate ( $q_0$ ) of H<sub>2</sub>O was found to be 0.29, which compares well to the value of 0.2 predicted by another AQP study (de Groot and Grubmuller, 2001). This difference can be attributed to the fact that the authors used a different (lower resolution) structure of AQP1 and a different water model. We found that  $q_0$  for D<sub>2</sub>O is  $\sim 7\%$  higher than for H<sub>2</sub>O, albeit with relatively large error bars (Table II).

Results of our osmotic pressure simulations are reported in Table III and Fig. 4 A for H<sub>2</sub>O, and in Table IV and Fig. 4 B for D<sub>2</sub>O. We found that the osmotic permeability of D<sub>2</sub>O ( $8.5 \times 10^{-14} \text{ cm}^3/\text{s}/\text{pore}$ ) is 15% lower than that of H<sub>2</sub>O ( $10.0 \times 10^{-14} \text{ cm}^3/\text{s}/\text{pore}$ ). This difference compares well with the experimentally measured difference of  $\sim 21\%$ . We could not compare the individual values of the osmotic permeabilities because of the experimental uncertainty in the number of the AQP1

channels per proteoliposome. The osmotic permeability of H<sub>2</sub>O  $10.0 \times 10^{-14} \text{ cm}^3/\text{s}/\text{pore}$  obtained in our MD simulations is similar to that predicted by another MD study where a value of  $7.1 \times 10^{-14} \text{ cm}^3/\text{s}/\text{pore}$  was reported (Zhu et al., 2004). In addition it also compares well with the experimentally measured unit osmotic conductance ( $p_f$ ) of  $11.7 \times 10^{-14} \pm 1.8 \times 10^{-14} \text{ cm}^3/\text{s}/\text{pore}$  reported by Zeidel et al. (1994). Since water moves in a single file fashion through the AQP1 channel, the  $p_f/p_d$  ratio should give the number of solute molecules lining the pore (Finkelstein, 1987). The calculated  $p_f/p_d$  ratios for H<sub>2</sub>O and D<sub>2</sub>O are 11.8 and 8.4, respectively. The  $p_f/p_d$  ratio of H<sub>2</sub>O is in good agreement with the value 11.9 predicted in Zhu et al. (2004) and 13.2 measured experimentally (Mathai et al., 1996).

In conclusion, a new TIP3P-HW model for D<sub>2</sub>O was developed for simulation of D<sub>2</sub>O transport through AQP1. This model reproduces the experimental differences observed in the density and the self diffusion coefficient of H<sub>2</sub>O vs. D<sub>2</sub>O. Both MD simulations and experimental measurements confirm that D<sub>2</sub>O and H<sub>2</sub>O permeate the AQP1 channel. The observed lower permeability of D<sub>2</sub>O is attributed to the lower self diffusion coefficient and higher viscosity of D<sub>2</sub>O compared with H<sub>2</sub>O. Our study showed that MD could accurately predict the decreased permeability of D<sub>2</sub>O in AQP1 in advance of experimental measurements. This study will be helpful for designing MD simulations to study permeation of solutes through AQP1 that are not easily amenable to experiments such as carbon dioxide, hydrogen sulfide, and oxygen.

We would like to thank Zuzana Valnickova, Jan Enghild, Niels Chr. Nielsen, and Astrid C. Sivertsen (University of Aarhus, Aarhus, Denmark) for providing us purified AQP1 for initial studies.

The authors gratefully acknowledge computer time provided by PSC grant MCB030021P. M.L. Zeidel and J.C. Mathai are supported by a grant from the National Institutes of Health, DK 43955. A.B. Mamonov and R.D. Coalson were supported by National Science Foundation grant CHE-0518044 and Army Research Office grant DADD19-02-1-0227.

Olaf S. Andersen served as editor.

Submitted: 25 April 2007

Accepted: 8 June 2007

TABLE IV

Results of applied pressure MD simulations for D<sub>2</sub>O

Applied pressure	Time	No. of D <sub>2</sub> O permeations	Flux	$p_f \times 10^{14}$
MPa	ns		D <sub>2</sub> O/ ns/ pore	cm <sup>3</sup> /s/pore
25	7	21	0.74	
50	22	126	1.4	
100	34	239	1.8	$8.5 \pm 0.45$
200	20	333	4.2	

## REFERENCES

- Allen, M.P., and D.J. Tildesley. 1987. *Computer Simulation of Liquids*. Clarendon Press; Oxford University Press, Oxford Oxfordshire, New York. 408 pp.
- Chakrabarti, N., E. Tajkhorshid, B. Roux, and R. Pomes. 2004. Molecular basis of proton blockage in aquaporins. *Structure*. 12:65–74.
- Chen, H., Y. Wu, and G.A. Voth. 2006. Origins of proton transport behavior from selectivity domain mutations of the aquaporin-1 channel. *Biophys. J.* 90:L73–L75.
- de Groot, B.L., T. Frigato, V. Helms, and H. Grubmuller. 2003. The mechanism of proton exclusion in the aquaporin-1 water channel. *J. Mol. Biol.* 333:279–293.
- de Groot, B.L., and H. Grubmuller. 2001. Water permeation across biological membranes: mechanism and dynamics of aquaporin-1 and GlpF. *Science*. 294:2353–2357.
- de Groot, B.L., D.P. Tieleman, P. Pohl, and H. Grubmuller. 2002. Water permeation through gramicidin A: desformylation and the double helix: a molecular dynamics study. *Biophys. J.* 82:2934–2942.
- Essmann, U., L. Perera, M.L. Berkowitz, T. Darden, H. Lee, and L.G. Pedersen. 1995. A smooth Particle Mesh Ewald Method. *J. Chem. Phys.* 103:8577–8593.
- Finkelstein, A. 1987. *Water Movement through Lipid Bilayers, Pores and Plasma Membranes*. John Wiley & Sons, Inc., New York. 228 pp.
- Fu, D., A. Libson, L.J. Miercke, C. Weitzman, P. Nollert, J. Krucinski, and R.M. Stroud. 2000. Structure of a glycerol-conducting channel and the basis for its selectivity. *Science*. 290:481–486.
- Grigera, J.R. 2001. An effective pair potential for heavy water. *J. Chem. Phys.* 114:8064–8067.
- Humphrey, W., A. Dalke, and K. Schulten. 1996. VMD: visual molecular dynamics. *J. Mol. Graph.* 14:33–38.
- Jorgensen, W., J. Chandrasekhar, and J. Madura. 1983. Comparison of simple potential functions for simulating liquid water. *J. Chem. Phys.* 79:926–935.
- Kale, L., R. Skeel, M. Bhandarkar, R. Brunner, A. Gursoy, N. Krawetz, J. Phillips, A. Shinozaki, K. Varadarajan, and K. Schulten. 1999. NAMD2: greater scalability for parallel molecular dynamics. *J. Comput. Phys.* 151:283–312.
- Karan, D.M., and R.I. Macey. 1980. The permeability of the human red cell to deuterium oxide (heavy water). *J. Cell. Physiol.* 104:209–214.
- MacKerell, A.D., D. Bashford, M. Bellott, R.L. Dunbrack, J.D. Evanseck, M.J. Field, S. Fischer, J. Gao, H. Guo, S. Ha, et al. 1998. All-atom empirical potential for molecular modeling and dynamics studies of proteins. *J. Physiol. Chem B.* 102:3586–3616.
- Mark, P., and L. Nilsson. 2001. Structure and dynamics of the TIP3P, SPC, and SPC/E water models at 298 K. *J. Physiol. Chem A.* 105:9954–9960.
- Mathai, J.C., S. Mori, B.L. Smith, G.M. Preston, N. Mohandas, M. Collins, P.C. van Zijl, M.L. Zeidel, and P. Agre. 1996. Functional analysis of aquaporin-1 deficient red cells. The Colton-null phenotype. *J. Biol. Chem.* 271:1309–1313.
- Mills, R. 1973. Self-diffusion in normal and heavy water in the range 1–45. *J. Phys. Chem.* 77:685–688.
- Miloshevsky, G.V., and P.C. Jordan. 2004. Water and ion permeation in bAQPI and GlpF channels: a kinetic Monte Carlo study. *Biophys. J.* 87:3690–3702.
- Murata, K., K. Mitsuoka, T. Hirai, T. Walz, P. Agre, J.B. Heymann, A. Engel, and Y. Fujiyoshi. 2000. Structural determinants of water permeation through aquaporin-1. *Nature*. 407:599–605.
- Nemethy, G., and H.A. Scheraga. 1964. Structure of water and hydrophobic bonding in proteins. IV. The thermodynamic properties of liquid deuterium oxide. *J. Chem. Phys.* 41:680–689.
- Neria, E., S. Fischer, and M. Karplus. 1996. Simulation of activation free energies in molecular systems. *J. Chem. Phys.* 105:1902–1921.
- Nielsen, S., J. Frokiaer, D. Marples, T.H. Kwon, P. Agre, and M.A. Knepper. 2002. Aquaporins in the kidney: from molecules to medicine. *Physiol. Rev.* 82:205–244.
- Roudier, N., J.M. Verbavatz, C. Maurel, P. Ripoché, and F. Tacnet. 1998. Evidence for the presence of aquaporin-3 in human red blood cells. *J. Biol. Chem.* 273:8407–8412.
- Scheiner, S., and M. Cuma. 1996. Relative stability of hydrogen and deuterium bonds. *J. Am. Chem. Soc.* 118:1511–1521.
- Sui, H., B.G. Han, J.K. Lee, P. Walian, and B.K. Jap. 2001. Structural basis of water-specific transport through the AQP1 water channel. *Nature*. 414:872–878.
- Tajkhorshid, E., P. Nollert, M.O. Jensen, L.J. Miercke, J. O’Connell, R.M. Stroud, and K. Schulten. 2002. Control of the selectivity of the aquaporin water channel family by global orientational tuning. *Science*. 296:525–530.
- Tredgold, R.H., and R. Jones. 1979. A study of gramicidin using deuterium oxide. *Biochim. Biophys. Acta.* 550:543–545.
- van der Spoel, D., P.J. van Maaren, and H.J.C. Berendsen. 1998. A systematic study of water models for molecular simulation: derivation of water models optimized for use with a reaction field. *J. Chem. Phys.* 108:10220–10230.
- Vidossich, P., M. Cascella, and P. Carloni. 2004. Dynamics and energetics of water permeation through the aquaporin channel. *Proteins*. 55:924–931.
- Weast, R. 1977. *CRC Handbook of Chemistry and Physics*. 64th Edition. CRC Press, Cleveland, OH. F-4.
- Yang, B., T. Ma, and A.S. Verkman. 2001. Erythrocyte water permeability and renal function in double knockout mice lacking aquaporin-1 and aquaporin-3. *J. Biol. Chem.* 276:624–628.
- Ye, R.G., and A.S. Verkman. 1989. Simultaneous optical measurement of osmotic and diffusional water permeability in cells and liposomes. *Biochemistry*. 28:824–829.
- Zeidel, M.L., S.V. Ambudkar, B.L. Smith, and P. Agre. 1992. Reconstitution of functional water channels in liposomes containing purified red cell CHIP28 protein. *Biochemistry*. 31:7436–7440.
- Zeidel, M.L., S. Nielsen, B.L. Smith, S.V. Ambudkar, A.B. Maunsbach, and P. Agre. 1994. Ultrastructure, pharmacologic inhibition, and transport selectivity of aquaporin channel-forming integral protein in proteoliposomes. *Biochemistry*. 33:1606–1615.
- Zhu, F., E. Tajkhorshid, and K. Schulten. 2004. Theory and simulation of water permeation in aquaporin-1. *Biophys. J.* 86:50–57.